Ultrasensitive and Indirect Electrochemical Detection of Sulfamethoxazole Using Ag₂O @ MWCNTs Nanocomposites Modified Glassy Carbon Electrode

Wenhao Zhang, Rui Li, Mingfang Zhu, Wen Zhou, Mushen Lai, Huanru Liang, Rongkun Zhu, Hongqing Ye*

College of Pharmacy, Guangdong Pharmaceutical University, Guangzhou higher education mega center, Guangzhou 510006, P.R.China
*E-mail: zhumfgy@126.com

The Ag₂O @ MWCNTs nanocomposites material was prepared via simple, one-step *situ precipitation* method using conventional reagent. The obtained Ag₂O @ MWCNTs was structurally characterized by scanning electron microscopy (SEM), fourier transform infrared spectroscopy (FTIR) and ultraviolet and visible spectrophotometry (UV–Vis). The functional GCE with Ag₂O @ MWCNTs exhibits good electrochemical performances with a pair of quasi-reversible redox peak. While sulfamethoxazole (SMX) can interact with Ag(I) to form Ag-SMX complex, which makes the concentrations of silver ion involved in the redox reaction decreased, thus reducing the redox peak of Ag₂O @ MWCNTs composites. The decreased oxidation peak current is found to be linear with the SMX concentrations from 0.02–100 nM and the detection limit was 4.06×10^{-12} M (S/N=3) by using DPV method. Furthermore, the proposed method demonstrated excellent selectivity, repeatability and reproducibility, and can be successfully applied for the SMX analysis in human serum.

1. INTRODUCTION

Sulfamethoxazole (SMX), Para-aminophthalamide derivative, is belonging to chemical synthesized antibiotics. The molecular size and charge distribution of sulfamethoxazole is similar to that of p-aminobenzoic acid (PABA), which hinders the synthesis of dihydrofolate by inhibiting the synthetase of dihydrofolate competitively[1], leading to bacterial nucleic acid synthesis obstacle thereby bacterial action inhibited, so SMX is a broad-spectrum antibacterial effect [2]. Thanks to its properties like low price, convenient to use, it is widely applied for clinical practice such as the

treatment of several infection diseases mainly treat urinary tract infection [3]. And sulfamethoxazole is also used in large quantities in veterinary medicines compared to other antibiotics [4-6]. In addition, it is used to prevent or treat systemic or local infections and is used in food additives or in drinking water for the treatment of various infections [7]. In general, SMX listed of class III carcinogens and the emergence of the drug-resistant bacteria during treatment has been reported [8]. The low solubility of sulfonamides plays a crucial role in toxicity as they accumulate in foods such as milk or meat, and SMX is one of the most extensively used sulfa drugs [9]. To ensure the human health, the European Commission has determined the maximum residue limit in edible tissue, including animal food and milk for human consumption [10].

Different methods have been proposed for the assay of SMX, including spectrophotometry[11-12], immunoassay methods[13-14], high performance liquid chromatography -mass spectrometry (HPLC-MS) and HPLC with ultraviolet detection[15-16], and electrochemical determination methods with various modified materials[17-18]. Most of these methods are direct determination, while indirect determination of SMX is rarely reported. Su group reported an indirect inhibitive immunoassay for the analysis of SMX[14], and the detection limit of SMX was 0.01 $\mu g\ L^{-1}$. Compared with other analytical methods, indirect electroanalytical determinations could be done at very low concentration. Besides, the indirect determination of SMX based on the nanocomposites modified glassy carbon electrode has not been reported.

Up till now, various nanostructured materials are widely used in electrochemical research. Metal oxide nanoparticles have attracted far-reaching attention because of their simple and green preparation method, low costs, high specific surface areas, super optical and electronic performance, high conductivities and catalytic activities. [19-22]. Among the metal oxide nanoparticles, silver oxide nanoparticles have become a promising electrode modified materials because of their excellent catalytic activity, unique electrical conductivity, relatively low price, high surface to volume ratio and good biocompatibility [23-24]. In order to overcome the irreversible agglomerates of the silver oxide nanoparticles, suitable substrate should be chosen. It is well known, multi-walled carbon nanotubes (MWCNT) is a good electrochemical modified materials [25], meanwhile, MWCNT is also a good substrate materials for metals and metal oxides nanoparticles owing to its large adsorption capacity and good electrocatalytic performance. Therefore, it is an effective strategy to constrction biosensors and electrochemical sensors based on the synergistic effect of the metal oxide and MWCNTs nanoparticles [26].

The present work aims the construction of an electrochemical sensor for applying the DPV to indirectly detect and quantify SMX in serum samples, based on the Ag$_2$O@MWCNTs through a simple synthesis route. The functionalized GCE with Ag$_2$O@MWCNTs (Ag$_2$O@MWCNTs / GCE) itself exhibits good electrochemical performances at the potential of 0.16 V, while SMX can interact with Ag(I) to form Ag-SMX complex to reduce the redox peak. The decreased oxidation peak is stable and the peak current values were linear to the concentration of SMX, so we can use indirect measurement to detect SMX accurately. The method is simple, reproducible and sensitivity to the determination of SMX in human serum samples.

2. EXPERIMENTAL

2.1 Chemical regents

Sulfamethoxazole (SMX), Ornidazole, Gatifloxacin, Streptomycin, Shafloxacin, Tinidazole, Lincomycin hydrochloride, Tetracycline hydrochloride, Levofloxacin and N, N-dimethylformamide (DMF) were purchased from Aladdin Reagent Co., Ltd. (Shanghai, China), Multi-walled carbon nanotubes (MWCNTs) were obtained from Suzhou Hengqiu technology Inc. (Jiangsu, China). Silver nitrate ($AgNO_3$) was supplied from China Chengdu Chemical Reagent Factory. Ammonium hydroxide was obtained from Sigma-Aldrich. All other chemicals were analytical grade and supplied from Tianjin Damao chemical reagent factory. Double-distilled water was used to configure determination aqueous solutions.

2.2 Instrumentation

All electrochemical experiments were operated on IGS 4030 electrochemical workstation (Guangzhou Ingsens Sensor Technology co., Ltd. China). A conventional three-electrode system was used, consisting of a bare glassy carbon electrode (GCE) or GCE with surface modified as working electrode, an Ag/AgCl/3.0 M KCl electrode and a platinum electrode were used as the reference and auxiliary electrode, respectively. The electrochemical measurements were performed at room temperature. Scanning electron microscopy (SEM) images were obtained using ZEISS LEO1530VP (Germany). The UV–Vis spectra were obtained by UV 2550 spectrophotometer (Shimadzu, Japan). The Fourier-Infrared spectra (FT-IR) were obtained by Spectrum 100 FT-IR Spectrometer (Perkin Elmer, U.S.A.).

2.3 Fabrication of Ag$_2$O @ MWCNTs nanocomposites and Ag$_2$O@MWCNTs / GCE

The method of *in situ* precipitation was to prepare as grown Ag_2O @ MWCNTs by vigorous mixing process from silver nitrate with ammonium hydroxide as the precipitating agent. 0.0425g silver nitrate was dissolved in 50.00 mL of deionized water. 0.0500g MWCNTs were immersed in the above solution. Then, the mixture solution was ultrasound for two hours until dispersed properly. The solution pH was slowly adjusted at 8.5 by dropping wise ammonium hydroxide, then it was stirred at 50 °C for 10.0 hours. After being stirred, the product was collected by centrifugation, followed by being rinsed for three times with ethanol and water,respectively. Subsequently, the solid precipitate was dried at 80 °C for 8.0 hours. The solid precipitation was presented as Ag_2O @ MWCNTs. And 5 mg of the solid powder was accurately accessed and dissolved in 5 mL of N-N-dimethylformamide for an electrode modification material. 10 μL Ag_2O @MWCNT solution was dripped onto the cleaned glassy carbon electrode and the modified GCE was dried with infrared lamp, then Ag_2O@MWCNTs / GCE was obtained.

3. RESULTS AND DISCUSSION

3.1 Ag₂O @ MWCNTs /GCE characterization

The morphology of MWCNT and Ag$_2$O @ MWCNTs were observed by scanning electron microscopy (SEM). It is clearly seen from Fig. 1B and the insetion of Fig.1B, irregular ball-shaped Ag$_2$O nanoparticles with diameters of about 20~30 nanometers dispersed uniformly on the tubular MWCNTs surface, which is different from that of the wrapped and agglomerated MWCNT in Figure 1A, indicating the formation of Ag$_2$O @ MWCNTs composites[27].
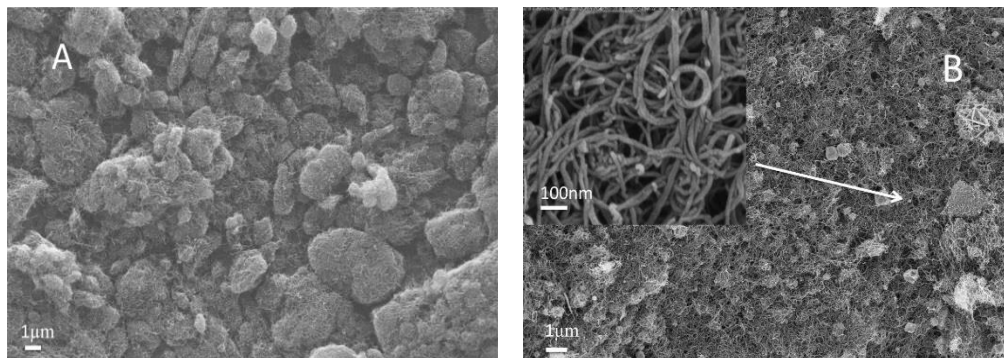

Figure 1. The SEM images of (A) MWCNT, (B) Ag$_2$O-MWCNT, the insertion of B is the enlarged figure.
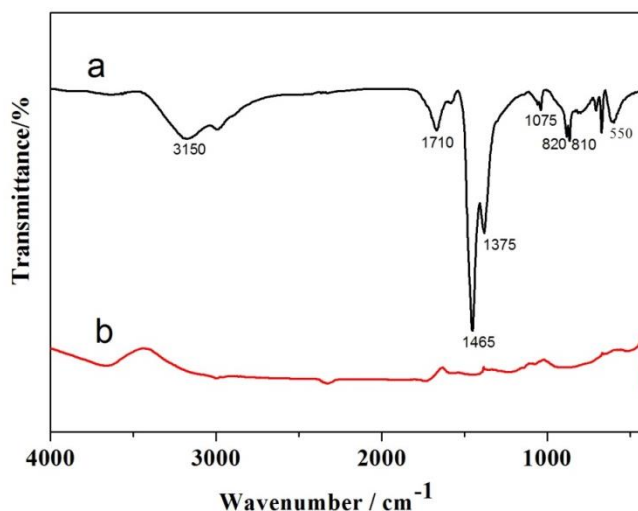

Figure 2. FTIR spectra of Ag$_2$O @ MWCNTs (a), MWCNTs (b).

FT-IR spectrum of Ag$_2$O@MWCNTs is presented in Fig.2. It represents several bands at 550 cm^{-1}, 810 cm^{-1}, 820 cm^{-1}, 1075 cm^{-1}, 1375 cm^{-1}, 1465 cm^{-1}, 1710 cm^{-1} and 3150 cm^{-1} in Fig.2a, which is consistent with the reported[27]. The observed bands at 550 cm^{-1} may be indicated Ag-O-Ag stretching vibration[28], the peaks at 810 cm^{-1},820 cm^{-1}, 1075 cm^{-1} arisen from multi-phonon processes in Ag$_2$O, 1375 cm^{-1}, 1465 cm^{-1} as the CO_2 stretching vibration, 3150 cm^{-1} and 1710 cm^{-1} for the H_2O stretching vibration, The bands at 1375 cm^{-1},1465 cm^{-1}, 1710 cm^{-1} and 3150 cm^{-1} are

appeared for the stretching vibration of absorbed water and carbon dioxide from atmosphere[28], as a result of the mesoporous nature of $Ag_2O@MWCNTs$ nanomaterials. The results indicated that the composites had been synthesized.

UV-vis spectroscopy of $Ag_2O@MWCNTs$ NPs and MWCNT were presented in Fig. 3. From Fig.3b and the insertion of Fig.3, it can be clearly seen that MWCNT shown an absorption peak at about 310 nm, and a broad absorption band around 278.0 nm to 311nm in the range between 200.0 and 800.0 nm wavelengths in Fig.3a, 311nm is attributed to the MWCNT and 278nm to the silver oxide nanoparticles [29]. The band-gap energy (Ebg) is calculated according to the maximum absorption band of $Ag_2O@MWCNTs$ nanoparticles and the equation is as follows [30],

$$Ebg = \frac{1240}{\lambda} \ (eV)$$

where Ebg is the band gap energy and λ_{max} presented the wavelength ($\sim$278.0 nm) of the $Ag_2O@MWCNTs$ nanoparticles. According to the above equation, Ebg is obtained to be about 4.4604 eV.
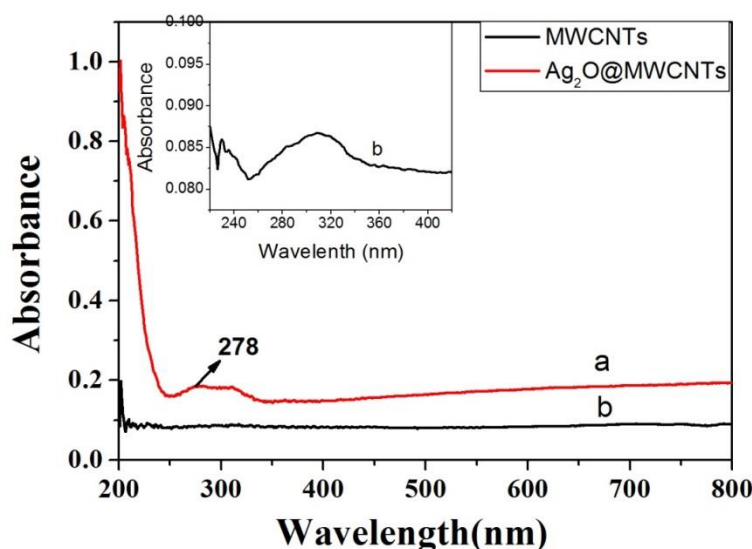

Figure 3. UV spectrum of the Ag_2O @ MWCNTs (a) and MWCNTs (b), the insetion is the enlarged figure of MWCNTs.

3.2 Electrochemical characterization of Ag_2O @ MWCNTs /GCE

The modified electrode was characterized using cyclic voltammetry (CV) and electrochemical impedance spectroscopy (EIS). The electrochemical behaviors of GCE, MWCNTs/GCE and $Ag_2O@MWCNTs$ /GCE in 0.1 M KCl solution, which contains 5 mM $K_3[Fe(CN)_6]$ and $K_4[Fe(CN)_6]$, were examined by CV (Figure 4A) and EIS (Figure 4B). The redox potential difference (ΔEp) on the GCE (a) was calculated to be 70 mV. In contrast with this, ΔEp on the MWCNTs/GCE (b) and $Ag_2O@MWCNTs$ /GCE (c) are almost the same. However, the redox peak currents change significantly from a to c. That is from 75μA increases to 80 μA and finally to 126 μA. This maybe that the silver oxide and MWCNTs can accelerate electronic transfer between the electrode and solution,

the Ag$_2$O@MWCNTs composite modified GCE performed the higher peak current than MWCNTs modified GCE, which indicates silver oxide is helpful to increase current and could play a significant role in it. Moreover, the result also shows that Ag$_2$O@MWCNTs / GCE had been prepared.
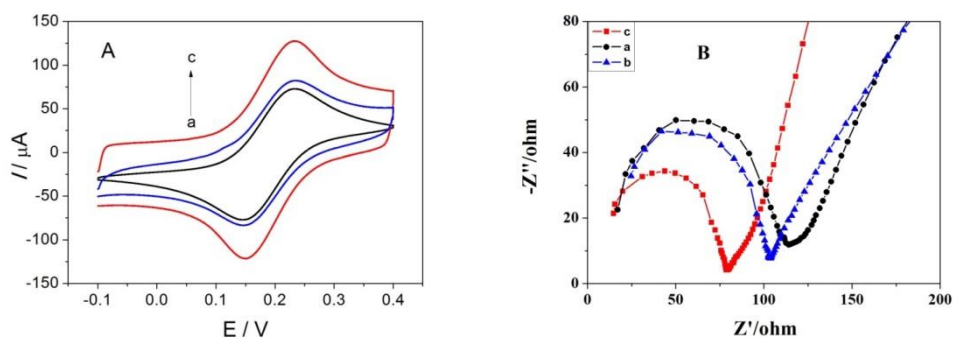

Figure 4. (A) CVs of 5.0 mM K$_4$Fe(CN)$_6$ $^{3-/4-}$ on GCE (a), MWCNTs /GCE (b), and Ag$_2$O @ MWCNTs /GCE (c) in 0.1 M KCl solution with the scan rate of 100 mV s^{-1}. (B) Nyquist plots of 5.0 mM [Fe (CN)$_6$]$^{3-/4-}$ on GCE (a), MWCNTs /GCE (b) and Ag$_2$O @ MWCNTs /GCE (c) in 0.1 M KCl . Frequency range: 100 kHz-0.1 Hz. Amplitude: 0.005 V.

Electrochemical impedance spectroscopy (EIS) can be used to probe the impedance feature of the modified electrodes surface. Fig. 4B shown the Nyquist plots of 5 mM [Fe(CN)$_6$]$^{3-/4-}$ on GCE (a), MWCNTs/GCE(b) and Ag$_2$O@MWCNTs /GCE(c) in 0.1 M KCl solution. In EIS, the semicircle segment observed at higher frequencies represents the electron-transfer resistance (Rct) [31]. The Rct value at the GCE(a), MWCNTs/GCE(b) and Ag$_2$O@MWCNTs /GCE(c) are 126 Ω. 102 Ω, 78 Ω respectively. This means that Ag$_2$O / MWCNTs composites have better electron transfer rate than MWCNTs, which may be due to the synergistic catalysis of Ag$_2$O and MWCNTs to provide a variety of conductive ways through MWCNTs tube like networks. These results further illustrated that Ag$_2$O@MWCNTs has been modified onto the GCE.

3.3 The electrochemical behavior of the Ag$_2$O@MWCNTs /GCE

The cyclic voltammograms of GCE and MWCNTs /GCE in PBS buffer solution (0.1 M, pH=7.4) do not show any obvious peaks (Fig.5A, curves a and b and the inset of Fig.5A) from the scan range of -0.2 V to 0.35 V at a scan rate of 100 mVs^{-1}, but a pair of redox peaks in PBS buffer solution (0.1 M, pH=7.4) at the Ag$_2$O@MWCNTs /GCE (Fig.5A, curve c), which peak positions are +0.17 V and -0.05 V, respectively. The peak at the potential of 0.17 V is assigned to the oxidation of Ag(0) to Ag(I), while the peak of -0.05 V is attributed to the reduction of Ag(I) to Ag(0)[23]. The electrochemical behaviors of SMX on GCE, MWCNTs/GCE and Ag$_2$O@MWCNTs/GCE were also studied in PBS buffer solution (0.1 M, pH=7.4). Figure 5B shows CV curves of GCE (Fig.5, curve a), MWCNTs/GCE (Fig.5, curve b) and Ag$_2$O@MWCNTs/GCE (Fig.5, curve c) in PBS solution containing 1 μM SMX. No redox peaks can be seen at the GCE and MWCNTs/GCE, indicating that t GCE and MWCNTs/GCE are no electrochemical activities in the range of scan potential.
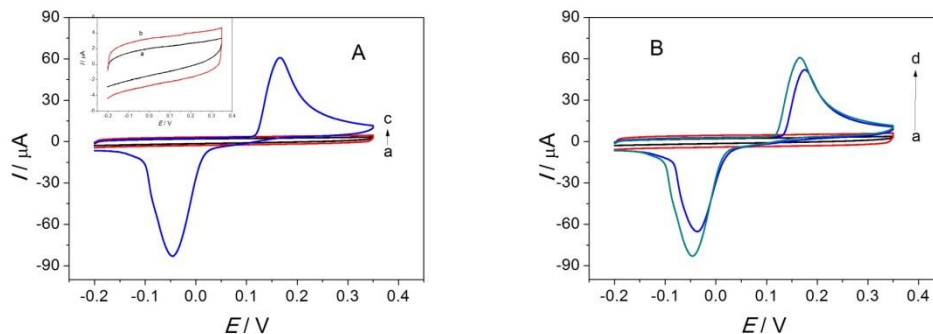
Figure 5. CVs of (A) GCE (a), MWCNTs /GCE (b) and Ag_2O @ MWCNTs /GCE (c) in 0.1M PBS (pH 7.4) solution; (B) CVs of GCE (a), MWCNTs /GCE (b) and Ag_2O @ MWCNTs /GCE (c) in 0.1M PBS (pH 7.4) solution with 1 μM SMX, and Ag_2O @ MWCNTs /GCE (d) in 0.1M PBS (pH 7.4) without SMX.

Nevertheless, the Ag_2O@MWCNTs/GCE (Fig.5B, curve c) demonstrate a pair of redox peaks at the potential of 0.175V and -0.038V, respectively. Compared with the Ag_2O@MWCNTs /GCE without SMX in solution (Fig.5B, curve d), the potential shifted slightly to the right and the redox current decreased.
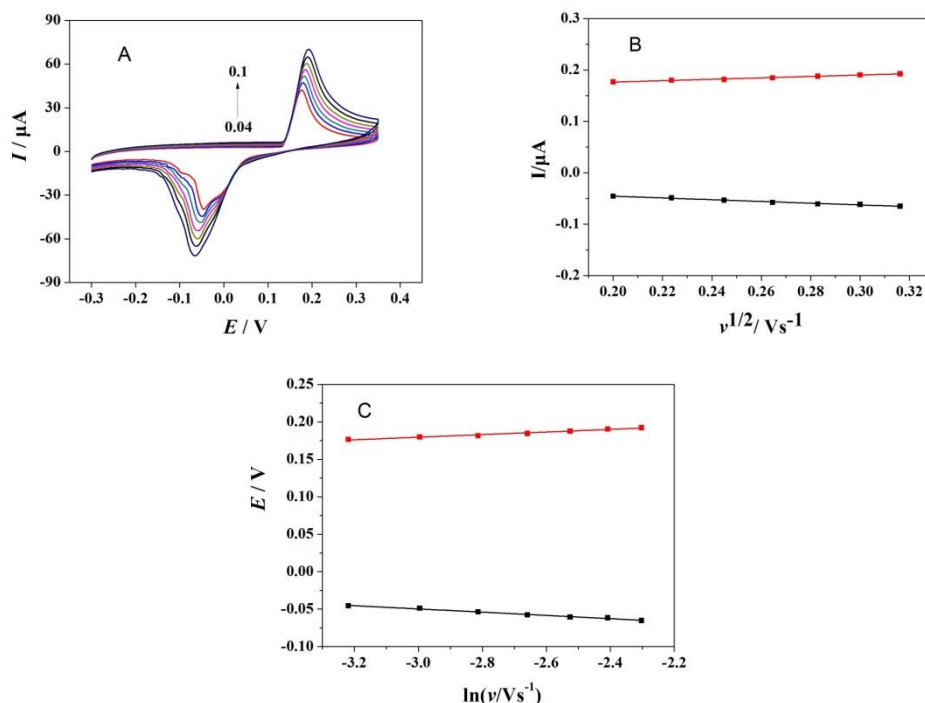

Figure 6. (A) CVs of Ag_2O @ MWCNTs /GCE in 0.1M PBS buffer solution with different scan rates: 40, 50, 60, 70, 80, 90, and 100 mVs^{-1}; (B) Plots of Ipa and Ipc vs. $v^{1/2}$; (C) Plots of Epa vs. ln$v$.

The reason may be that silver ions react to SMX to form Ag-SMX complex to hinder the electron transfer on the surface of the electrode, and the peak height of the Ag_2O redox peaks are lowered[32-33]. Since the decreased oxidation peak currents is related to the amount of the added SMX, and the oxidation peak was more stable than reduction peak, thus the oxidation peaks can be used to the determination of SMX.

The effect of scan rate of $Ag_2O@MWCNTs$ /GCE was discussed with CV. Figure 6A displayed that as the scan rate increased from 0.04 Vs^{-1} to 0.1 Vs^{-1}, E_{pa} moved positively and E_{pc} moved negatively, and the peak currents increased linearly with the square root of the scan rate (Fig. 6B), and the linear regression equations were $I_{pa} = 0.1374v^{1/2} + 0.1487$, R = 0.9955; and $I_{pc} = -0.1702v^{1/2} - 0.0117$, R = 0.9931; It is stated clearly that the electrode reaction was a diffusion control process.

Furthermore, it is found that there is a linear relationship between the redox peak potential and natural logarithm of scan rate (Fig. 6C) with the linear regression equations were: $E_{pa} = 0.0174 \ln v + 0.2317$, R = 0.9893; and $E_{pc} = -0.0217 \ln v - 0.1148$, R = 0.9940, respectively. According to the Laviron[34] equations:

$$E_{pa} = E^0 + m\left[0.78 + \ln(D^{1/2}K_s^{-1}) - 0.5\ln m\right] + \frac{m}{2}\ln v, \; m = \frac{RT}{(1-\alpha)nF} \quad (1)$$

$$E_{pc} = E^0 - m'\left[0.78 + \ln(D^{1/2}K_s^{-1}) - 0.5\ln m\right] + \frac{m'}{2}\ln v, \; m' = \frac{RT}{\alpha nF} \quad (2)$$

$$\log K_s = \alpha \log(1-\alpha) + (1-\alpha)\log \alpha - \log\frac{RT}{nFv} - \frac{(1-\alpha)\alpha F\Delta E_p}{2.3RT} \quad (3)$$

Where α is the charge transfer coefficient, n is the number of electrons transferred during the redox process, F refers to the Faraday constant, and K_s is the electron transfer rate constant. Using the above equations, α, n, and K_s were calculated to be 0.44, 1.32, and $0.21s^{-1}$, respectively.

3.4 The influence of experimental conditions

The pH will affect the activity of the antibiotics, so we investigated the electrochemical response of SMX between the pH range of 6.0–8.0, and the difference of oxidation peak current (Δi_p) is the basis of judging pH value. Here $\Delta i_p = i_0 - i$, where i_0 is the oxidation peak current of the $Ag_2O@MWCNTs$ /GCE in PBS, and i refers to the oxidation peak current of different SMX concentrations in PBS solution on $Ag_2O@MWCNTs$ /GCE. The highest Δi_p obtained at pH 7.4 (Fig. 7A), demonstrating that the $Ag_2O@MWCNTs$ /GCE is more active at pH 7.4, on the other hand, it is also suggested that pH 7.4 is the best pH for the formation of SMX-Ag complex. So pH 7.4 was used in all the experiments.

Meanwhile, the influence of response time on the Δi_p is investigated. The Δi_p increased and reached plateaus at 4 s (Figure 7B). Hence, the response time is selected as 4 s. To achieve good response of SMX, the volume of $Ag_2O@MWCNTs$ modification solution was varied from 1 to 7 μL. As it is shown in Fig. 7C, the difference oxidation peak current of Ag_2O were increased with increasing the $Ag_2O@MWCNTs$ solution volume from 1 to 3 μL, but decreases constantly up to 7 μL. Thus 3 μL was chosen for further experiments.
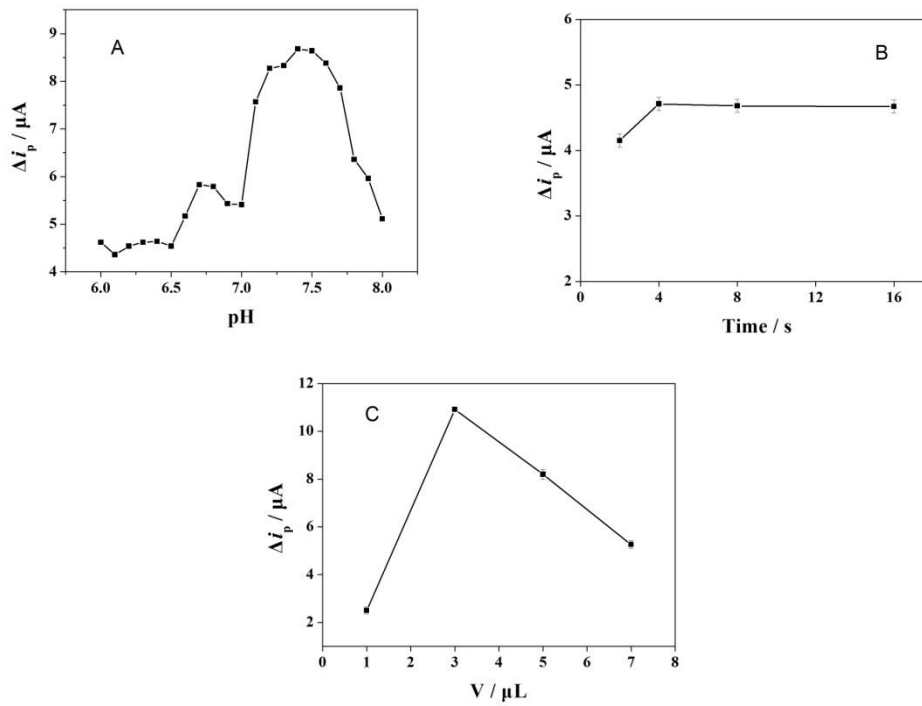
Figure 7. (A) The relationship between Δi_p and various pH from 6.0 to 8.0 at the Ag$_2$O @ MWCNTs /GCE in 0.1M PBS with 1μM SMX. (B) Effect of reaction time between SMX (1μM) and Ag-$_2$O @ MWCNTs /GCE in 0.1M PBS (pH 7.4).(C) various modification amount of Ag$_2$O @ MWCNTs in 0.1M PBS (pH 7.4) with 1μM SMX.

3.5 Calibration curvefor the derermination of SMX

Figure 8A displays the DPV responses of SMX with different concentrations from 0 to 0.10 μM under the optimized experimental conditions in PBS (pH 7.4) at Ag$_2$O@MWCNTs/GCE.
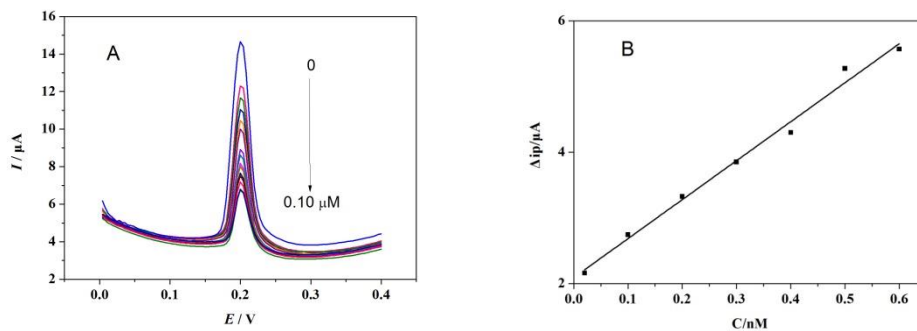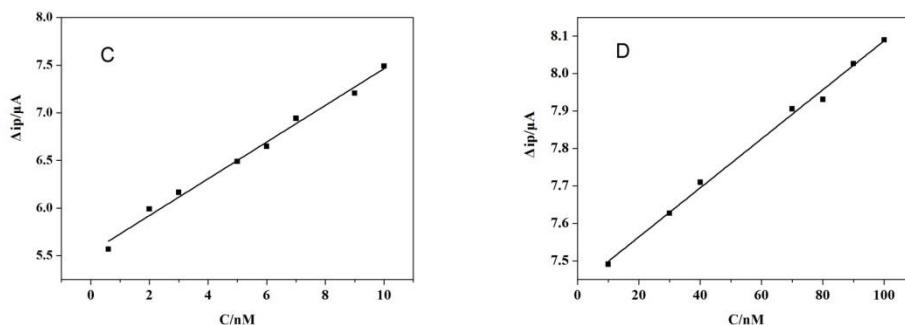
Figure 8. (A) DPV curves of the SMX with different concentrations from 0 to 0.10 μM at the Ag$_2$O@MWCNTs /GCE in 0.1 M PBS (pH7.4); (B) Linear plot for different concentrations of SMX from $2.0 \times 10^{-11} \sim 6.0 \times 10^{-10}$ M. (C) Linear plot for different concentrations of SMX from $6.0 \times 10^{-10} \sim 1.0 \times 10^{-8}$ M. (D) Linear plot for different concentrations of SMX from $1.0 \times 10^{-8} \sim 1.0 \times 10^{-7}$ M.

Table 1. Comparison of different modified electrode for the SMX detection

Electrode Material	Method	Linear range (μM)	LOD (μM)	Reference
Ag-MWCNT/MTOAC/GCE	DPV	0.05-70	10	[35]
TYR-AuNPs-SPCEs	Amperometric	20-200	22.6	[36]
PDA-MIP film	Amperometric	0.8-170	0.8	[17]
The anti-SMX Ab/CeO$_2$ -CHIT / GCE	DPV	0.002-2	1.28×10^{-3}	[37]
Paraffin / MWCNT - SbNPs	DPV	0.1-0.7	0.024	[38]
	DPV	1.0–10.0	3.8×10^{-2}	[39]
MWCNt/PBnc/SPE				
Ag$_2$O@ MWCNTs	DPV	2×10^{-5}-0.1	4.06×10^{-6}	This work

Ag-MWCNT/MTOAC/GCE: silver-filled multi-walled carbon nanotube and methyltrioctyl ammonium chloride modified glassy carbon electrode; TYR-AuNPs-SPCEs: Tyrosinase cross-linking gold nanoparticles modified screen-printed carbon electrodes; PDA-MIP film: molecularly imprinted polydopamine films; The anti-SMX Ab/nanoCeO$_2$-CHIT/GC:CeO$_2$-chitosan (CHIT)-modified nanocomposite immobilizing anti-sulfamethoxazole (SMX) polyclonal antibody modified glass carbon (GC) electrode; Paraffin/MWCNT-SbNPs: Multi-walled carbon nanotubes modified with antimony nanoparticles paraffin composite. MWCNt/PBnc/SPE: multiwalled nanotubes decorated with Prussian blue nanocubes modified screen-printed electrode

The oxidation peak current was found to decrease with the increase in the SMX concentration. In addition, linear relationships were found between Δip and SMX concentrations, the first SMX concentrations range from $2.0 \times 10^{-11} \sim 6.0 \times 10^{-10}$ M with a correlation coefficient of 0.9953 (Fig. 8B). And the following SMX concentration ranges: $6.0 \times 10^{-10} \sim 1.0 \times 10^{-8}$ M, and $1.0 \times 10^{-8} \sim 1.0 \times 10^{-7}$ M with correlation coefficients of 0.9958, and 0.9979, respectively (Figs. 8 C, and D, respectively). The linear

equations are $\Delta i_p = 5931.6c + 2 \times 10^{-6}$, $\Delta i_p = 192.75c + 6 \times 10^{-6}$, $\Delta i_p = 6.5485c + 7 \times 10^{-6}$, respectively. the lowest detection limit is 4.06×10^{-12} M (S/N=3).

Comparison with other electrochemical methods, the proposed sensor in this work showed an indirect voltammetric detection of SMX with broader detection ranges and super lower LOD, the method provided in this paper for the determination of SMX is compared with other methods as shown in Table 1.

3.6 Interference studies

To study the selectivity of Ag$_2$O@MWCNTs /GCE, when the detection of SMX, some foreign substances with the same concentration (1 μM) of Ornidazole (ODZ), Gatifloxacin (GTX), Streptomycin (STM), Shafloxacin (SFX), Tinidazole (TDZ), Lincomycin hydrochloride (LCM), Tetracycline hydrochloride (TCL) and Levofloxacin (LFX), were added. It can be seen from Figure 9A, the Δi_p in case of these interfering substances were found to vary within ±3% of that measured in case of SMX only. It suggested that the presence of these foreign species did not interfere with the determination of SMX.

3.7 The stability, repeatability, and reproducibility of the nanocomposite
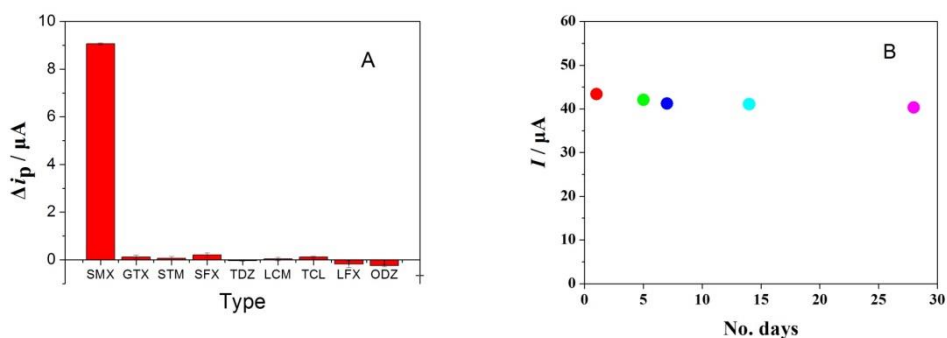

Figure 9. (A) The selectivity of the modified electrode for SMX detection. (B) Stability investigation of the modified electrode by DPV. Conditions: 0.1 M PBS (pH=7.4), Storing at room temperature for 28 days.

To study the stability of the modified electrode, the durable stability of Ag$_2$O@MWCNTs /GCE has been evaluated for 28 days, the peak current decreased by 7.06%, indicating that the Ag$_2$O@MWCNTs /GCE had good stability (Fig. 9B).

To examine repeatability features of the modified electrode, cyclic voltammograms have been recorded using Ag$_2$O@MWCNTs/GCE for 15 consecutive cycles at 100 mVs^{-1} scan rate without SMX (Fig.10A) and with 1μM SMX (Fig.10B). Considering the result, the repeatability of both blank solution and the solution with SMX is very well.
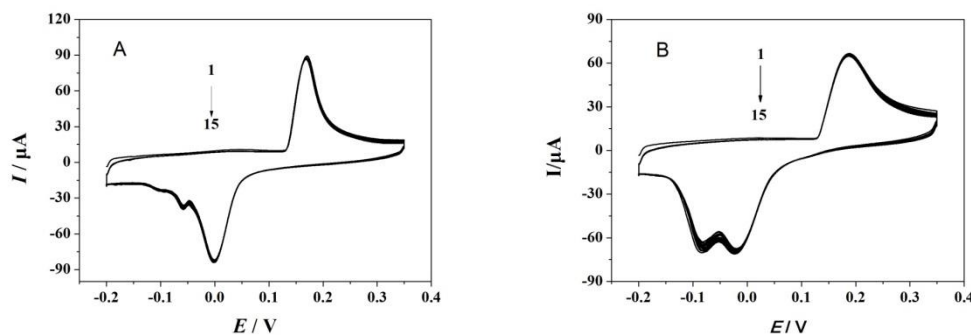
Figure 10. CVs of Ag$_2$O@MWCNTs /GCE for 15 consecutive cycles at a scan rate of 100 mV s^{-1} in 0.1 M PBS (pH=7.4) (A) without SMX and (B) with 1μM SMX.

The reproducibility of the Ag$_2$O@MWCNTs/GCE was evaluated by measuring 1 μM SMX in 0.1 M PBS solution (pH 7.4) with five different electrodes. The RSD is 2.04%, it revealed that the method has good reproducibility.

3.8 The application of Ag$_2$O@MWCNTs /GCE to serum samples

To estimate the reliability and practicality of Ag$_2$O@MWCNTs /GCE, the sensor was used for the detection of SMX in samples of human serum obtained from the Outpatient Department of the Hospital Affiliated with Guangdong Pharmaceutical University. Before the experiment, the serum samples were diluted 50-fold using 0.1 M PBS (pH 7.4), and then detected different concentrations of SMX using the standard addition method. The results were listed in Table 2, the recoveries were 96.27%-100.2% and the relative standard deviations (RSD) were 0.85% ~ 2.5%. Thus, the proposed method can be used to the determination of SMX in human serum.

Table 2. Determination of SMX in serum by DPV method using Ag$_2$O@MWCNTs/GCE (n=3).

Sample	Analyte	Added (μM)	Founded (μM)	Recovery (%)	RSD (%)
		0.010	0.010	100.0	1.0
Serum	SMX	0.050	0.049	98.0	1.5
		0.100	0.096	96.0	2.8

4. CONCLUSIONS

The results presented above demonstrate that the Ag$_2$O @ MWCNTs modified electrodes exhibit a ultrasensitive electrochemical behavior for the indirect determination of SMX. The designed nanocomposite materials involved a simple preparation and the sensor was easymodification. Moreover, the Ag$_2$O@MWCNTs/GCE have the advantages of high selectivity, sensitivity and reproducibility. In light of the antibiotic abuse in the worldwide and SMX associated listed of class III

carcinogens and the emergence of the drug-resistant bacteria, simple and accurate analysis of SMX is very useful. Hence, the presented chemical modification sensor has the potential to be practically applied for the determination of SMX in human serum.

References

1. P. Drillia, S. N. Dokianakis, M. S. Fountoulakis, M. Kornaros, K. Stamatelatou, G. Lyberatos, *J. Hazard. Mater.*, 122 (2005) 259.
2. J. Xu, Y. Xu, H. Wang, C. Guo, H. Qiu, Y. He, Y. Zhang, X. Li, W. Meng, *Chemosphere*, 119 (2015) 1379.
3. I. N. Dias, B. S. Souza, J. H. O. S. Pereira, F. C. Moreira, M. Dezotti, R. A. R. Boaventura, V. J. P. Vilar, *Chem. Eng. J.*, 247 (2014) 302.
4. L. E. Redding, S. Lavigne, H. Aceto, R. Nolen-Walston, *Prev. Vet. Med.*, 168 (2019) 66.
5. M. B. Ahmed, J. L. Zhou, H. H. Ngo, W. Guo, *Sci. Total Environ.*, 532 (2015) 112.
6. L. Hu, P. M. Flanders, P. L. Miller, T. J. Strathmann, *Water Res.*, 41 (2007) 2612.
7. L. Zhao, Y. H. Dong, H. Wang, *Sci. Total Environ.*, 408 (2010) 1069.
8. H. E. Eldesouky, X. Li, N. S. Abutaleb, H. Mohammad, M. N. Seleem, *Int. J. Antimicrob. Agents*, 52 (2018) 754.
9. W. Haasnoot, M. Bienenmann-Ploum, U. Lamminmäki, M. Swanenburg, H. van Rhijn, *Anal. Chim. Acta*, 552 (2005) 87.
10. J. Shen, F. Xu, H. Jiang, Z. Wang, J. Tong, P. Guo, S. Ding, *Anal. Bioanal. Chem.*, 389 (2007) 2243.
11. M. C. Mahedero, T. G. Diaz, S. G. Pascual, *Talanta*, 57 (2002) 1.
12. S. M. Sabry, *Anal. Lett.*, 39 (2006) 2591.
13. H. Hoffmann, S. Baldofski, K. Hoffmann, S. Flemig, C. P. Silva, V. I. Esteves, F. Emmerling, U. Panne, R. J. Schneider, *Talanta*, 158 (2016) 198.
14. P.-P. Tang, Z.-F. Luo, J.-B. Cai, Q.-D. Su, *Chinese J. Anal. Chem.*, 38 (2010) 1019.
15. W. Jansomboon, S. K. Boontanon, N. Boontanon, C. Polprasert, C. Thi Da, *Food Chem.*, 212 (2016) 635.
16. D.C.G. Bedor, T.M. Gonçalves, M.L.L. Ferreira, C.E.M.D. Sousa, A.L. Menezes, E.J. Oliveira, D.P. D. Santana, *J. Chromatogr. B*, 863 (2008) 46.
17. A. Turco, S. Corvaglia, E. Mazzotta, P. P. Pompa and C. Malitesta, *Sens. Actuators*, *B*, 255 (2018) 3374.
18. L. F. Sgobbi, C. A. Razzino, S. A. S. Machado, *Electrochim. Acta*, 191 (2016) 1010.
19. G. Mohan Kumar, P. Ilanchezhiyan, C. Siva, A. Madhankumar, T. W. Kang, D. Y. Kim, *Int. J. Hydrogen Energy*, 45 (2020) 391.
20. M. Ishizaki, H. Fujii, K. Toshima, H. Tanno, H. Sutoh and M. Kurihara, *Inorg. Chim. Acta*, 502 (2020) 119345.
21. K. Ponprapakaran, R. H. Subramani, R. Baskaran, R. Anbarasan, *Synth. Met.*, 232 (2017) 144.
22. M. Kenarkob, Z. Pourghobadi, *Microchem. J.*, 146 (2019) 1019.
23. V. H. R. Azevedo, J. L. da Silva, N. R. Stradiotto, *J. Electroanal. Chem.*, 845 (2019) 57.
24. J. W. Zhang, R. F. Li, L. Yao, Z. X. Wang, W. X. Lv, F. Y. Kong, W. Wang, *J. Electroanal. Chem.*, 823 (2018) 1.
25. A. R. Boccaccini, J. Cho, J. A. Roether, B. J. C. Thomas, E. Jane Minay, M. S. P. Shaffer, *Carbon*,

    44 (2006) 3149.
26. A. Merkoci, M. Pumera, X. Llopis, B. Pe´rez, M. D. Valle, S. Alegret, *Trends Anal. Chem.*, 24 (2005) 826.
27. S. B. Khan, M. M. Rahman, H. M. Marwani, A. M. Asiri, K. A. Alamry, *J. Taiwan Inst. Chem. E.*, 45 (2014) 2770.
28. G. I. N. Waterhouse, G. A. Bowmaker, J. B. Metson, *Phys. Chem. Chem. Phys.*, 3 (2001) 3838.
29. M. M. Rahman, H. M. Marwani, F. K. Algethami, A. M. Asiri, S. A. Hameed, B. Alhogbi, *Environ. Nanotechnol. Monit. Manage.*, 8 (2017) 73.
30. M. Prathap Kumar, G. A. Suganya Josephine, A. Sivasamy, *J. Mol. Liq.*, 242 (2017) 789.
31. D. Manoj, R. Saravanan, J. Santhanalakshmi, S. Agarwal.,V. K. Gupta, R. Boukherroub, *Sens. Actuators, B*, 266 (2018) 873.
32. J. H. Bormio Nunes, R. E. F. de Paiva, A. Cuin, W. R. Lustri, P. P. Corbi, *Polyhedron*, 85 (2015) 437.
33. J. Sundberg, H. Witt, L. Cameron, M. Hakansson, J. Bendix, C. J. McKenzie, *Inorg. Chem.*, 53 (2014) 2873.
34. R. S. Nicholson, I. Shain, *Anal. Chem.*, 36 (1964) 706.
35. Yari, A. and A. Shams, *Anal. Chim. Acta*, 1039 (2018) 51.
36. L. D. T. Román, M. A. Alonso-Lomillo, O. Domínguez-Renedo, M. J. Arcos-Martínez, *Sens. Actuators, B*, 227 (2016) 48.
37. M. Cai, L. Zhu, Y. Ding, J. Wang, J. Li, X. Du, *Mater. Sci. Eng. C*, 32 (2012) 2623.
38. I. Cesarino, V. Cesarino, M. R. V. Lanza, *Sens. Actuators, B*, 188 (2013) 1293.
39. L. F. Sgobbi, C. A. Razzino, S. A. S. Machado, *Electrochim. Acta*, 191 (2016) 1010.